ChemPubSoc Europe

DOI: 10.1002/cbic.201500572

CHEMBIOCHEM Full Papers

Unprecedented Utilization of Pelargonidin and Indole for the Biosynthesis of Plant Indole Alkaloids

Anne-Christin Warskulat, Evangelos C. Tatsis, Bettina Dudek, Marco Kai, Sybille Lorenz, and Bernd Schneider*[a]

To the memory of Dr. sc. nat. Hartmut Böhm

Nudicaulins are a group of indole alkaloid glycosides responsible for the color of yellow petals of *Papaver nudicaule* (Iceland poppy). The unique aglycone scaffold of these alkaloids attracted our interest as one of the most unusual flavonoid-indole hybrid structures that occur in nature. Stable isotope labeling experiments with sliced petals identified free indole, but not tryptamine or L-tryptophan, as one of the two key biosynthetic precursors of the nudicaulin aglycone. Pelargonidin was identified as the second key precursor, contributing the polyphenolic unit to the nudicaulin molecule. This finding was inferred from the temporary accumulation of pelargonidin glycosides in the petals during flower bud development and a drop at the point in time when nudicaulin levels start to increase. The precursor-directed incorporation of cyanidin into a new 3′-hydroxynudicaulin strongly supports the hypothesis that anthocyanins are involved in the biosynthesis of nudicaulins.

Introduction

Many plant indole alkaloids are highly bioactive natural products.[1] Vincristine and vinblastine from *Catharanthus roseus* are among the most prominent examples, because they are important medical drugs in cancer therapy.[2,3] The indole structure is also a building block of a multitude of synthetic compounds[4] that are not only used as pharmaceutical products but are also broadly applied in various technical branches.[5] The *Catharanthus* alkaloids and other natural monoterpene indole alkaloids are biosynthesized from tryptamine and secologanin, an iridoid glycoside, to form strictosidine.[6,7]

Apart from monoterpenes, few alternative building blocks have been reported to be involved in indole alkaloid biosynthesis. Flavonoid derivatives, for example, are rarely utilized for that purpose. Yuremamine, a natural product from the South American entheogenic plant *Mimosa tenuiflora*[8] and the Thai medicinal plant *Trigonostemon reidioides*,[9,10] was, to the best of our knowledge, the first reported natural indole alkaloid containing a flavonoid-derived unit. The nudicaulins from *Papaver nudicaule L.*,[11] *P. alpinum*, and *Meconopsis cambrica*[12] also belong to the class of flavonoidal indole alkaloids. The diastereomeric aglycones[13] of nudicaulins I and II are each composed of an indole unit fused to a polyphenolic scaffold, and the molecules are each decorated with three partly malonylated β-glucose units.

Because of the unprecedented structures and obscured biosynthesis of the nudicaulins, the data mining of transcriptome databases for candidate biosynthetic genes and biochemical approaches to search for the enzyme(s) catalyzing their formation was unfortunately not promising. Therefore, a retro-biosynthetic study using $^{13}CO_2$ as a metabolic tracer was performed.[14] In this recent work, both the indole and the phenolic parts of the nudicaulin molecule were shown to originate from shikimate. Overall, it has been concluded that the unique hexacyclic nudicaulin skeleton is the result of the biochemical fusion of an indole moiety with a flavonoid-like C_6-C_3-C_6 unit of phenylpropanoid/polyketide biogenetic origin. The indole biosynthetic pathway is well established[15] and proceeds through anthranilate, *N*-(5-phosphoribosyl)anthranilate as the substrate for indole-3-glycerol phosphate synthase, forming indole-3-glycerol phosphate, and, further downstream, indole, L-tryptophan, and tryptamine. The principal question of whether or not indole, L-tryptophan, or tryptamine could act as the key precursor of the indole part of nudicaulins was not determined by the retro-biosynthetic study and therefore remained to be answered in this work.

Like the indole pathway, the phenylpropanoid/polyketide pathway is well established.[16,17] It is interesting in this context that some kaempferol derivatives and gossypitrin co-occur with nudicaulins in the yellow petals of *P. nudicaule*.[11] Moreover, the nudicaulins and the kaempferols in these petals are identically glycosylated and malonylated. Identical acylated carbohydrate units are attached not only to the mentioned aglycones, but also to pelargonidin in the red cultivar of *P. nudicaule*.[18] Hence, several constituents of the flavonoid pathway

[a] *Dr. A.-C. Warskulat, Dr. E. C. Tatsis, B. Dudek, Dr. M. Kai, S. Lorenz, Dr. B. Schneider*
Max Planck Institut für chemische Ökologie
Hans Knöll Strasse 8, 07745 Jena (Germany)
E-mail: schneider@ice.mpg.de

Supporting information for this article is available on the WWW under http://dx.doi.org/10.1002/cbic.201500572.

might potentially act as key precursors of the nudicaulins. Thus, another aim of this work was to obtain experimental evidence about which of them could function as a precursor of the non-indolic part of the nudicaulin structure.

Here we report the mass spectrometric and NMR analytical results of classical and retro-biosynthetic stable isotope labeling experiments and provide data from precursor-directed biosynthetic (PDB) experiments that strongly support the pathway proposed in this paper. In addition, we show that the time-dependent disappearance of pelargonidin derivatives in maturing petals of yellow *P. nudicaule* is correlated with a rise in the nudicaulin level. This finding indicates that pelargonidin derivatives could function as the key precursors that cyclize with their indolic counterpart.

Results and Discussion

Development of an experimental system for administering labeled precursors to *P. nudicaule*

Hydroponic supply is usually considered a promising way to administer isotope-labeled precursors successfully to plants. In *Papaver*, however, the latex leaking from the vascular system at the cut site of the plant material prevents absorption of supplied precursors. Therefore, the $^{13}CO_2$-pulse/chase labeling of intact *P. nudicaule* plants[14] was put forward as an elegant method to let them take up the labeled precursor from the atmosphere and circumvent the absorption issues of a hydroponic system. However, though successful in many respects, the retro-biosynthetic experiment using $^{13}CO_2$ as a general precursor prevented the drawing of conclusions about the two key precursors from the indole and phenylpropanoid/polyketide pathways that finally undergo fusion to form the nudicaulin molecules.

Hence, an alternative system for administering labeled precursors to *P. nudicaule* had to be established. Suspensions of sliced petals were considered an interesting alternative to whole plants or hydroponic systems. Firstly, however, the yellow petals had to be verified as the site of nudicaulin biosynthesis. To this end, a retro-biosynthetic experiment was performed, this time with [$^{13}C_6$]glucose as a general precursor and sliced petals as plant material. If the nudicaulin biosynthetic pathway were to exist in the petals, the labeling patterns would be expected to be comparable to those obtained on incubating intact plants in an atmosphere containing $^{13}CO_2$. Indeed, the results exhibited identical labeling patterns of nudicaulin I aglycone (Scheme 1) and nudicaulin II aglycone (not shown) from the experiments with $^{13}CO_2$[14] and [$^{13}C_6$]glucose, although the ^{13}C abundances found in the two experiments for some building blocks were quite different. It was inferred from this result that the entire machinery of nudicaulin biosynthesis, starting from primary metabolites, must be present in the yellow petals of *P. nudicaule*. No translocation of advanced biosynthetic precursors from other plant parts to the petals is necessary to produce nudicaulins. Hence, incubating sliced petals in an aqueous suspension was confirmed to be a suitable system for feeding labeled precursors to *P. nudicaule*. Because the isotopologue profiles of nudicaulins generated from [$^{13}C_6$]glucose closely resembled the profiles observed from incubation with $^{13}CO_2$, which have been discussed earlier,[14] the results of this [$^{13}C_6$]glucose experiment are summarized here only briefly, to demonstrate which building blocks are contributing to the nudicaulin scaffold. In the indole unit, a coupling pattern consistent with an origin from shikimate (six carbon atoms, C-14 to C-19) and phosphoribosyl pyrophosphate (two carbon atoms, C-2 and C-13) was observed. Shikimate also serves as the precursor of ring f (six carbon atoms, C-1′ to C-6′), whereas phosphoenol pyruvate contributes three carbon atoms (C-3, C-11, C-12) through the phenylpropanoid pathway. Ring a (C-4 to C-9) originates from three acetate/malonate units, which seem to be condensed to the polyketide starter—*p*-coumaroyl-CoA—to form a chalcone- or flavonoid-type inter-

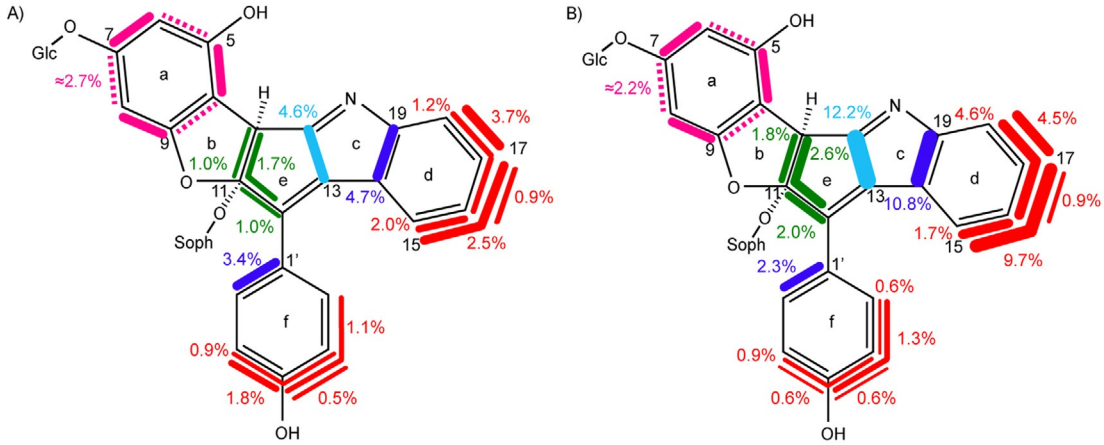

Scheme 1. Isotopologue profiles of nudicaulin I obtained from ^{13}C NMR-based retro-biosynthetic experiments with *P. nudicaule*. Full bars in the structures indicate doubly and triply ^{13}C-labeled isotopologues, and the widths and numbers show their relative molar abundances (see also Table S3). Dashed bars in ring a indicate isotopologues generated by alternative closure of ring b. The colors of the bars indicate the isotopologues derived from different biosynthetic pathways. Glc: β-glucosyl. Soph: β-sophorosyl. A) Nudicaulin I obtained from petals of intact plants incubated with $^{13}CO_2$.[14] B) Nudicaulin I obtained from sliced petals incubated with [$^{13}C_6$]glucose.

mediate. Thus, the general pathway and the biosynthetic origins of all carbon atoms of the nudicaulin aglycone have been confirmed.

Administration of indole pathway precursors

Because the nudicaulin aglycones each consist of indole and phenolic parts, the two key molecular entities that undergo fusion to form the molecule had to be identified. Therefore, labeled precursors were administered to the suspension of sliced petals, and their incorporation into the nudicaulin skeleton was studied by NMR and MS to establish direct precursor–product relationships.

Firstly, labeled indole pathway precursors—namely, [ring-$^{13}C_6$]anthranilic acid, [2-^{13}C]indole, L-[$^{13}C_{11}$]tryptophan, and [$^{13}C_{10}$]tryptamine—were probed. As shown by NMR and MS, the administration of [ring-$^{13}C_6$]anthranilic acid enhanced the ^{13}C NMR signals of C-14 to C-19 (Figure 1C, Figure S10 in the Supporting Information). The ^{13}C,^{13}C coupling satellites in the ^{13}C NMR spectrum and the $[M+H+6]^+$ ion in the mass spectrum (Figure 1B) indicated that the aromatic ring of anthranilic acid was incorporated as a whole, a finding consistent with the indole pathway. Feeding experiments with [^{15}N]anthranilic acid resulted in MS spectra displaying an increase in the $[M+H+1]^+$ signal, thus suggesting that the amine nitrogen atom of anthranilic acid acts as the source of N-1 of the nudicaulins (Figure S11).

As shown by the enhanced relative intensity of the isotope peak *m/z* 873 in the mass spectrum, labeled nudicaulins were synthesized during the incubation of sliced petals of *P. nudicaule* with [2-^{13}C]indole (Figure 2B). The enhanced signal in the ^{13}C NMR spectrum indicated that this label was located specifically at C-2 of the molecule (Figure 2C).

The NMR and mass spectra of nudicaulin samples obtained from the administration of L-[$^{13}C_{11}$]tryptophan and [$^{13}C_{10}$]-tryptamine did not display isotope enrichment in any of the replicated experiments. Hence, we conclude that the incorporation of these two labeled compounds did not take place

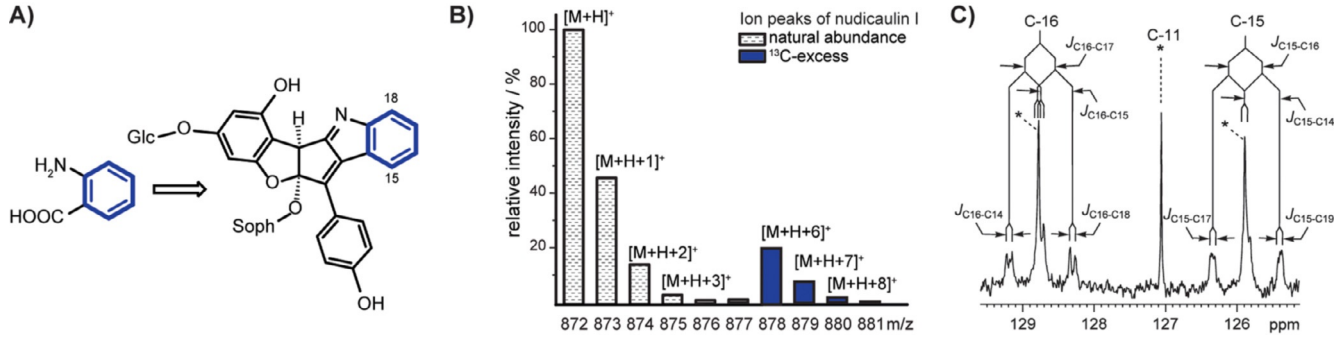

Figure 1. ^{13}C NMR spectroscopic and mass spectrometric detection of specific incorporation of the intact aromatic ring of [ring-$^{13}C_6$]anthranilic acid into nudicaulin I. A) Illustration of the precursor–product relationship between anthranilic acid and nudicaulin I. Bold blue bonds indicate contiguous ^{13}C-labeling. Glc: β-glucosyl. Soph: β-sophorosyl. B) Relative intensities of molecular and isotopic ion peaks in the mass spectrum of nudicaulin I (see also Figure S8 and Table S4). The ^{13}C excess of the peak at *m/z* 878 $[M+H+6]^+$ confirms the incorporation of the C_6 unit. C) A partial ^{13}C NMR spectrum (125 MHz, CD_3OD) showing signals of C-11, C-15, and C-16 (for the full spectrum, see Figure S10). ^{13}C,^{13}C coupling satellites with $^1J_{C15,C14}$, $^1J_{C15,C16}$, $^1J_{C16,C15}$, $^1J_{C16,C17} \approx 56$–58 Hz and $^2J_{C15,C13}$, $^2J_{C15,C17}$, $^2J_{C16,C14}$, $^2J_{C16,C18} \approx 9$ Hz indicate the ^{13}C-enrichment of adjacent carbon positions (signal overlap prevents exact extraction of *J* values; see Table S5). Asterisks indicate central signals of C-15 and C-16 and the signal of a naturally abundant carbon atom (C-11).

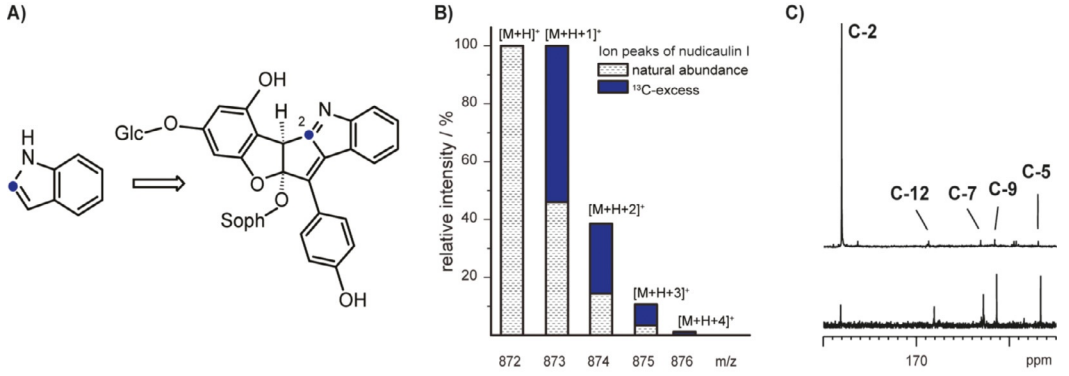

Figure 2. ^{13}C NMR spectroscopic and mass spectrometric detection of specific incorporation of the intact aromatic ring of [2-^{13}C]indole into nudicaulin I. A) Illustration of the precursor–product relationship between indole and nudicaulin I. ^{13}C-Labeled positions are marked with ●. Glc: β-glucosyl, Soph: β-sophorosyl. B) Relative intensities of molecular and isotopic ion peaks in the mass spectrum of nudicaulin I. The ^{13}C excess of the peak at *m/z* 873 $[M+H+1]^+$ confirms the incorporation of indole containing one ^{13}C atom (Figure S12 and Table S7). C) Upper spectrum: a partial ^{13}C NMR spectrum (175 MHz, CD_3OD) showing the enhanced signal of C-2 and natural-abundance signals of C-5, C-7, C-9, and C-12. Lower spectrum: partial reference spectrum of nudicaulin I. For full ^{13}C NMR spectra, see Figure S14.

during the incubation with sliced *P. nudicaule* petals under the experimental conditions used.

PDB experiment to probe the indole pathway

Not only have PDB experiments been used to generate new natural-product-like compounds with potential biological activity, but they also represent suitable approaches for investigating biosynthetic pathways and probing for the specificity or promiscuity of biosynthetic enzymes.[19] Fluorinated compounds are of special interest in this context because of the ease of their analytical traceability.

The suitability of PDB experiments for the study of nudicaulin biosynthesis was demonstrated by administering different anthranilic acid derivatives to *P. nudicaule* petal suspensions (Table 1). Of the unnatural anthranilic acid derivatives, 4-fluoroanthranilic acid, 5-hydroxyanthranilic acid, and 5-methylanthranilic acid were incorporated into the nudicaulin derivatives with corresponding substitutions in the indole unit.

A biosynthetic experiment with 5-fluorotryptamine was not successful (data not shown). This lack of incorporation supported the result of the experiment with [$^{13}C_{10}$]tryptamine: namely, that this biogenetic amine likely is not part of the nudicaulin biosynthesis pathway.

Table 1. PDB experiments to demonstrate the incorporation of unnatural anthranilic acid derivatives into nudicaulin derivatives. The products were analyzed by UPLC-MS (ESI) (extracted ion chromatograms).

Substrate		Product[a]	
4-fluoroanthranilic acid	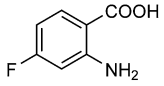	$C_{41}H_{44}FNO_{20}$ *m/z* 889.24	**1**
6-fluoroanthranilic acid	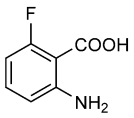	$C_{41}H_{44}FNO_{20}$ *m/z* 889.24	n.d.[b]
5-hydroxyanthranilic acid	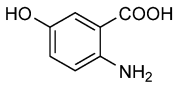	$C_{41}H_{45}NO_{21}$ *m/z* 887.25	**2**
3-hydroxyanthranilic acid	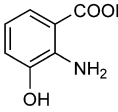	$C_{41}H_{45}NO_{21}$ *m/z* 887.25	n.d.
5-methylanthranilic acid	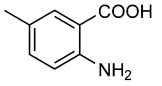	$C_{42}H_{47}NO_{20}$ *m/z* 885.27	**3**

[a] Structures of compounds **1** - **3**.
17-fluoronudicaulin (**1**):
R^1 = H, R^2 = F
16-hydroxynudicaulin (**2**):
R^1 = OH, R^2 = H
16-methylnudicaulin (**3**):
R^1 = CH_3, R^2 = H

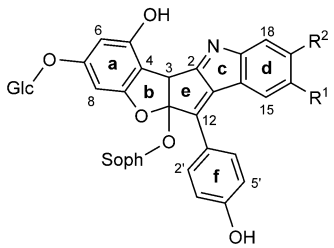

[b] n.d.: product not detected.

Administration of phenylpropanoid/plant polyketide pathway precursors

The administration of L-[$^{13}C_9$]phenylalanine to sliced *P. nudicaule* petals resulted in enhanced isotope ion signal *m/z* 881 $[M+H+9]^+$ of the nudicaulin aglycone; this suggested that all carbon atoms of the phenylpropanoid skeleton had been incorporated. The enhancement of ion signals *m/z* 873, 874, and 875 above the natural abundance indicated some scrambling of the ^{13}C-label due to vigorous amino acid metabolism. However, the significant ^{13}C-enrichment of C-3, C-11, and C-12, and also of ring f (C-1′ to C-6′), was shown by enhanced signals and especially by the ^{13}C,^{13}C coupling patterns in the ^{13}C NMR spectra of nudicaulins, as shown in Figure 3, panel B for nudicaulin I. Thus, the ^{13}C NMR data indicated that the entire carbon skeleton of the labeled phenylpropanoid had been incorporated into the target compound.

The presence of a hydroxy group in position C-4′ of ring f raised the question of whether this functionality is incorporated together with an already hydroxylated precursor or later in the nudicaulin biosynthesis. Because nudicaulins without a 4′-OH group are unknown, early hydroxylation—that is, of the aromatic amino acid (L-phenylalanine→L-tyrosine) or of phenylpropanoid acids (cinnamic acid→*p*-coumaric acid)—could reasonably be hypothesized. Indeed, labeling experiments detected incorporation of L-[2-^{13}C]tyrosine (Figure 4) and *p*-[2-^{13}C]-coumaric acid into the nudicaulins, thus indicating precursor–product relationships in both cases. Unfortunately, the limited amount of labeled nudicaulin obtained from experiments with L-[2-^{13}C]tyrosine was insufficient to demonstrate specific incorporation of ^{13}C into the quaternary C-11 position by means of ^{13}C NMR. However, the enhanced relative intensity of >50% of *m/z* 873 in the mass spectrum could not entirely be explained by scrambling of the single ^{13}C-label. The low incorporation rate for *p*-[2-^{13}C]coumaric acid (Figure S29 and Table S15) might be due to diminished uptake of the precursor into the sliced petals and/or enzymatic channeling or flux into flavonol biosynthesis. According to these results, the hydroxy group in ring f very likely is introduced early in nudicaulin biosynthesis and not only after the skeleton has been completed.

The polyketide origin of the carbon atoms in ring a was probed by using [$^{13}C_2$]acetate as a precursor. The ^{13}C–^{13}C bond labeling of C-4/C-5, C-6/C-7, and C-8/C-9 indicates that ring a is indeed generated from three acetate units through C–C bond formation between C-4 and C-9, and confirms the involvement of the plant polyketide pathway in nudicaulin biosynthesis (Figure 5). Bond labeling of C-5/C-6, C-7/C-8, and C-9/C-4 due to alternative cyclization (C–C bond formation between C-4 and C-5) was also observed (not shown in Figure 5 for simplification; see Figure S32 and Table S17). The oxygenation positions at C-5, C-7, and C-9 are consistent with the origin of the C_2 units from acetate.

Petal pigmentation during flower development

Price et al.[20] had already observed the red pigmentation of immature petals, still covered by the sepals in the bud of the

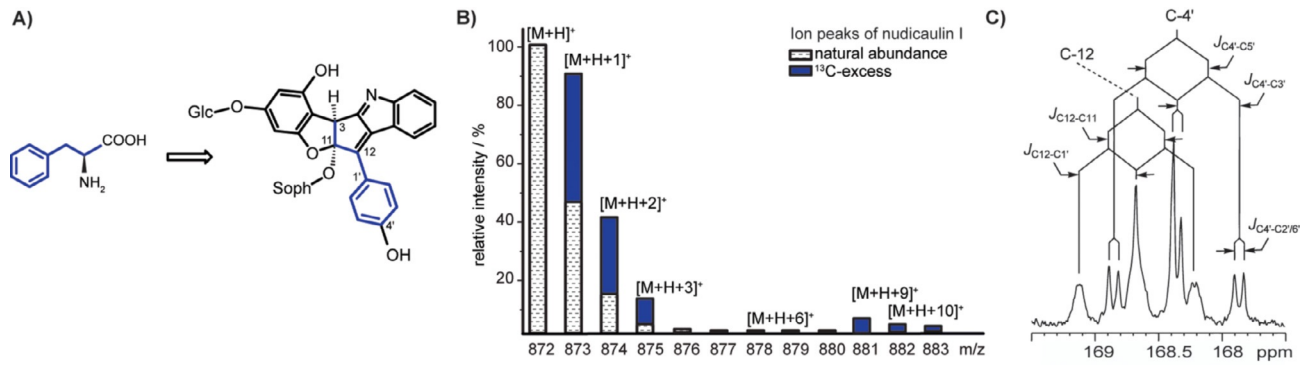

Figure 3. ^{13}C NMR spectroscopic and mass spectrometric detection of specific incorporation of the intact carbon skeleton of L-[$^{13}C_9$]phenylalanine into nudicaulin I. A) Illustration of the precursor–product relationship between L-phenylalanine and nudicaulin I. Blue bonds indicate contiguous ^{13}C-labeling. Glc: β-glucosyl. Soph: β-sophorosyl. B) Relative intensities of molecular and isotopic ion peaks in the mass spectrum of nudicaulin I (see also Figure S25 and Table S12). The enhanced relative intensity of the peak at *m/z* 881 $[M+H+9]^+$ confirms the incorporation of the C_9 skeleton. C) A partial ^{13}C NMR spectrum (125 MHz, CD_3OD) showing the signals of C-12 and C-4′ (for full spectrum see Figure S27). ^{13}C,^{13}C coupling satellites with $^1J_{C12,C11}=58$ Hz, $^1J_{C12,C1'}=54$ Hz, $^1J_{C4',C3'}=^1J_{C4',C5'}=62$ Hz, and $^2J_{C4',C2'/C6'}=9$ Hz indicate ^{13}C-enrichment of adjacent carbon positions (Table S13).

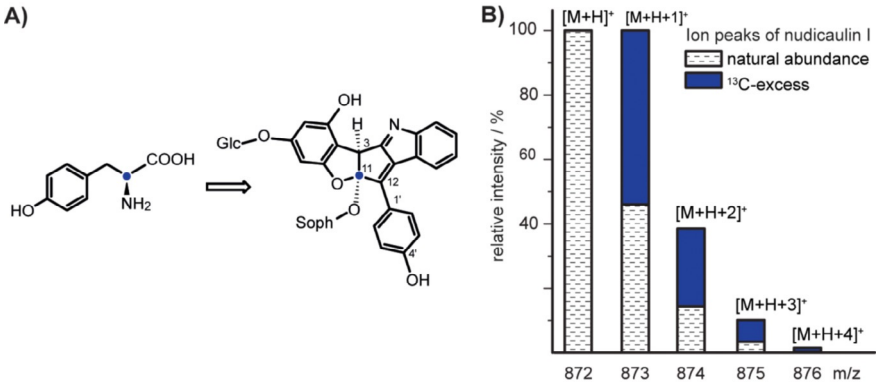

Figure 4. Mass spectrometric detection of L-[2-^{13}C]tyrosine incorporation into nudicaulin I. A) Illustration of the precursor–product relationship between L-tyrosine and nudicaulin I. ^{13}C-Labeled carbon positions are marked with ●. Glc: ß-glucosyl. Soph: β-sophorosyl. B) Relative intensities of molecular and isotopic ion peaks in the mass spectrum of nudicaulin I. The high ^{13}C excess of the isotope ion peak at *m/z* 873 $[M+H+1]^+$ indicates the incorporation of L-tyrosine into the nudicaulin molecule (see also Figure S28 and Table S14).

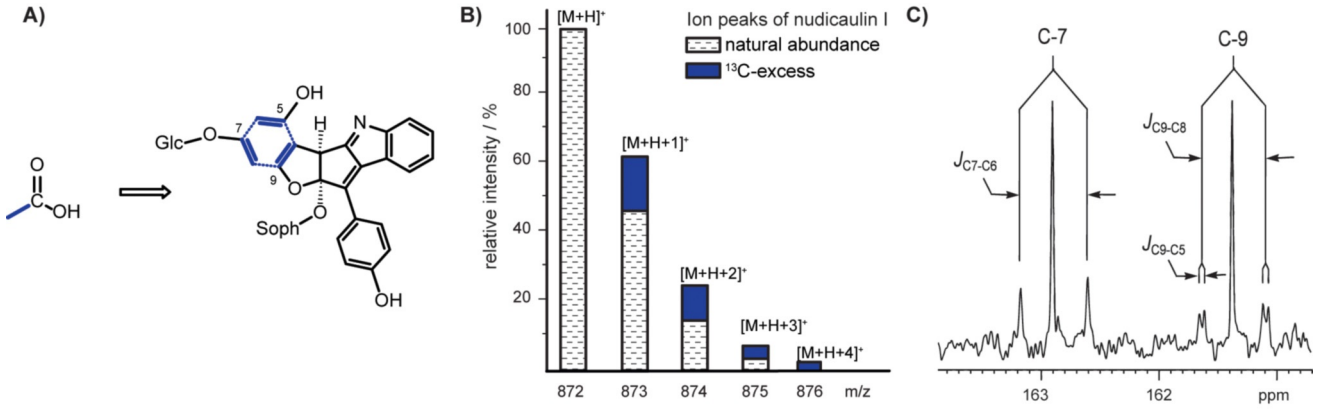

Figure 5. ^{13}C NMR spectroscopic and mass spectrometric detection of specific incorporation of [$^{13}C_2$]acetate into nudicaulin I. A) Illustration of the precursor–product relationship between acetate and nudicaulin I. Blue bonds indicate contiguous ^{13}C-labeling. Glc: β-glucosyl. Soph: β-sophorosyl. B) Relative intensities of molecular and isotopic ion peaks in the mass spectrum of nudicaulin I. The ^{13}C excesses of peaks at *m/z* 874 $[M+H+2]^+$ and *m/z* 876 $[M+H+4]^+$ confirm the incorporation of C_2 units (see also Figure S30 and Table S16). C) Partial ^{13}C NMR spectrum (125 MHz, CD_3OD) showing the signals of C-7 and C-9 (for the full spectrum see Figure S32). ^{13}C,^{13}C coupling satellites with $^1J_{C7,C6}=^1J_{C9,C8}=71$ Hz and $^2J_{C9,C5}=5$ Hz (Table S17) indicate the ^{13}C-enrichment of adjacent carbon positions.

yellow-blooming *P. nudicaule* cultivar, in 1939. These petals (Figure 6 A) change color during their development inside the closed buds. In the early stages of growth, the petals appear almost white. Then a slightly red pigmentation starts to develop and gradually intensifies until the petals obtain a deep red color. HPLC analysis of the extracts showed that the levels of

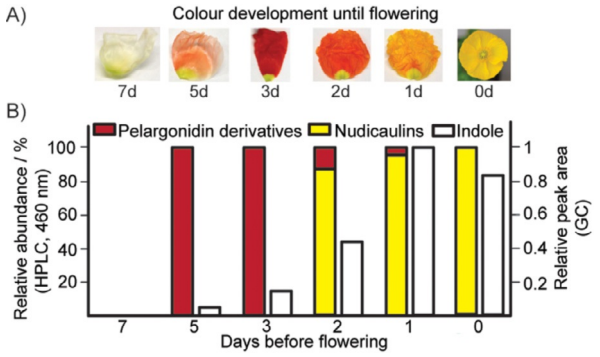

Figure 6. Development of petal pigmentation and levels of pelargonidin derivatives and nudicaulins in extracts of the yellow *P. nudicaule* cultivar inside the bud (days 1 to 5) prior to flowering. A) Pictures of petals inside the bud during flower development and opened flower. B) Relative abundances of pelargonidin derivatives, nudicaulins, and indole in petal extracts (see also Figures S23 and S33).

pelargonidin glycosides increased simultaneously, thus suggesting a correlation between the pelargonidin derivatives and the red pigmentation. The nudicaulins are not detectable in the early stages of development, and later their absorption is obscured by the intense red color of the pelargonidin derivatives. During further petal development, the red pigment fades and the yellow color of the nudicaulins becomes dominant, consistently with the HPLC data for the extracts (Figure 6 B; see also Figure S33). Finally, after the opening of the flowers, pelargonidin derivatives are no longer detectable and the nudicaulins alone dictate the appearance of the petals of yellow *P. nudicaule*.

The occurrence of indole in petals correlates with the formation of nudicaulins in blooming flowers of *P. nudicaule*

The successful incorporation of [2-^{13}C]indole into nudicaulins and the lack of incorporation of L-[$^{13}C_{11}$]tryptophan and [$^{13}C_{10}$]-tryptamine are unexpected results, so further data to support the role of free indole as an ultimate nudicaulin precursor were required. The successful incorporation of [2-^{13}C]indole into nudicaulins in the yellow-blooming cultivar also raised the question of the production of detectable indole levels in these petals. Indole was indeed found in the extracts by GC-MS analyses. The levels of indole increased during development until one day before flowering and then slightly dropped in blooming flowers (Figures 6, S23, and S24). This indole decrease might occur due to the consumption of the compound during the nudicaulin biosynthesis.

Precursor-directed administration of cyanidin and delphinidin

The decreasing levels of pelargonidin derivatives during the petal development, occurring along with the accumulation of nudicaulins, suggested that these anthocyanins act as biosynthetic precursors in nudicaulin formation. Unfortunately, labeling experiments were not feasible because pelargonidin and its derivatives were unavailable in labeled form. Instead, cyanidin and delphinidin were considered as alternative biosynthetic probes because the products of their incorporation would be distinguishable from nudicaulins. This is because the nudicaulins naturally occurring in the petals of *P. nudicaule* each possess a hydroxy group in the 4′-position of the phenylpropanoid-derived phenyl ring. With the exception of gossypitrin, no 3′,4′-dihydroxy substitution (catechol moiety) or 3′,4′,5′-trihydroxy substitution of phenolics has so far been detected in this plant,[11] probably because corresponding precursors are not utilized in the biosynthesis of the nudicaulins or do not exist in *P. nudicaule*. Hence, in the latter case, the successful incorporation into nudicaulins of a precursor possessing such an unusual substitution pattern would strongly indicate that the suggested pathway proceeds through an anthocyanidin.

Therefore, PDB experiments were performed by administering cyanidin and delphinidin to suspensions of sliced petals. After incubation for two days, the petals were extracted, and the extracts were subjected to selected ion monitoring mass spectrometric (SIM-MS) analysis. In the sample obtained from incubation with cyanidin, the signal at *m/z* 887.25 was consistent with the mass of a nudicaulin derivative ($C_{41}H_{45}NO_{21}$) possessing an additional hydroxy group, presumably in the 3′-position of ring f (Scheme 2). The molecular ion at *m/z* 887.25 was not detected in the petal extracts of control plants, thus making the natural occurrence of such a nudicaulin derivative implausible. However, no delphinidin incorporation into the nudicaulin scaffold was detected. In summary, the incorporation of cyanidin into nudicaulins strongly suggests that an anthocyanidin is involved in the nudicaulin biosynthesis pathway. According to the consistent substitution patterns of nudicaulins and pelargonidin derivatives, especially the 4′-OH group, this anthocyanidin can only be pelargonidin.

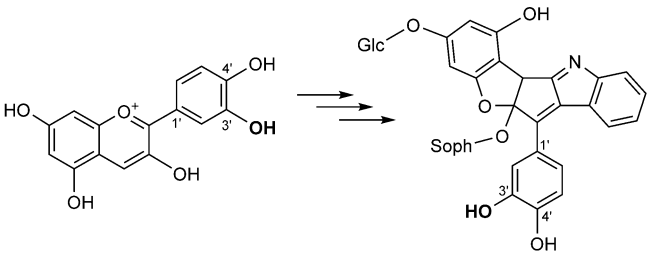

Scheme 2. Conversion of cyanidin into 3′-hydroxynudicaulin as inferred from SIM-MS analysis of an extract obtained from PDB experiments with sliced petals of *P. nudicaule*. The additional OH group is shown in bold. Glc: β-glucosyl. Soph: β-sophorosyl.

Conclusions

Previously reported pulse/chase labeling experiments with $^{13}CO_2$ in *P. nudicaule* and retro-biosynthetic interpretation of NMR and MS data established the biogenetic origin of nudicaulins from two biosynthetic routes: namely, the indole and the plant polyketide pathways. However, which of the specific intermediates of the two pathways combine to form the nudicaulin skeleton could not be inferred from the $^{13}CO_2$ study. Therefore, different strategies were employed here to provide further evidence about nudicaulin biosynthesis.

Overall, the administration of stable isotope precursors—and, more specifically, the use of [$^{13}C_6$]glucose—has revealed that the de novo biosynthesis of nudicaulin occurs in situ in *P. nudicaule* petals. The total ^{13}C-enrichment of nudicaulin obtained from ^{13}C-labeled precursors is given in Table 2.

Table 2. ^{13}C-Labeled precursors of the nudicaulin aglycone and their corresponding ^{13}C-enrichment calculated from mass spectra.

Precursor	Total ^{13}C-enrichment [%][a]	Precursor	Total ^{13}C-enrichment [%][a]
[$^{13}C_6$]glucose	3.3	[ring-$^{13}C_6$]anthranilic acid	16.9
[2-^{13}C]indole	56.1	L-[$^{13}C_9$]phenylalanine	11.3
L-[2-^{13}C]tyrosine	56.8	*p*-[2-^{13}C]coumaric acid	4.7
[$^{13}C_2$]acetate	13.4		

[a] Related to the number of ^{13}C-labeled positions.

In contrast with the known examples of ergot and monoterpene indole alkaloids, the conventional administration of stable isotope-labeled precursors identified free indole but not tryptamine or L-tryptophan as the most probable key precursor of the nudicaulins from the indole biosynthetic route. The observed temporary accumulation of pelargonidin glycosides in the petals during flower development—before these disappeared in favor of nudicaulins— indicated a precursor–product relationship between those pigments. This finding was strongly supported by the precursor-directed incorporation of cyanidin into a new 3′-hydroxynudicaulin. Thus, pelargonidin (or its glycosides) can be considered to serve as an intermediate (or intermediates) of the biosynthesis of nudicaulins (Scheme 3). These results were surprising because, to the best of our knowledge, both the utilization of pelargonidin and that of free indole are unprecedented in indole alkaloid biosynthesis and, generally, in natural product chemistry. Another result of this study is the generation of new unnatural nudicaulin derivatives by PDB experiments.

A hypothetical mechanistic model for the fusion of indole and pelargonidin is proposed in Scheme 4. Electrophilic aromatic substitution of indole at C-3 could start the fusion with pelargonidin. A second electrophilic aromatic substitution of indole at C-2 would lead to another C–C bond and close the central five-membered ring, and could be followed by a dehydrogenation step. Spontaneous acetalization could close ring b and explain the occurrence of (3*S*,11*R*)- and (3*R*,11*S*)-nudicaulin

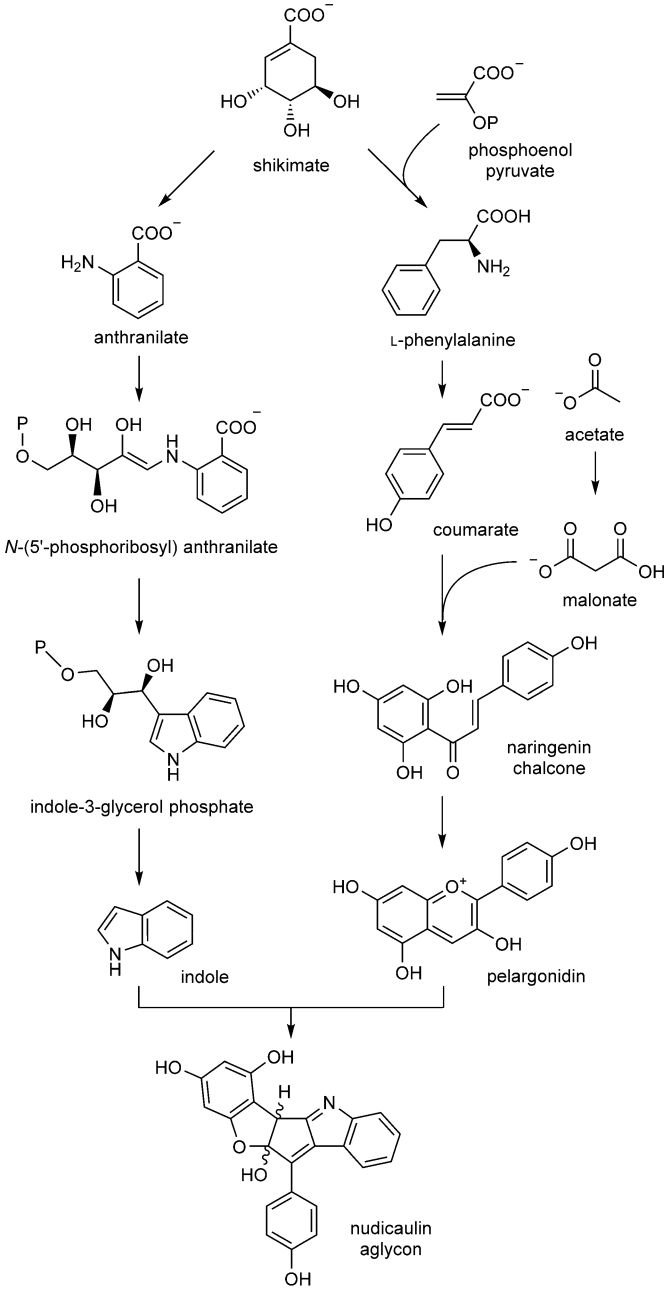

Scheme 3. Biosynthetic pathways leading to the nudicaulin aglycone through the two key precursors: indole and pelargonidin.

diastereomers. The final deprotonation could finish the biosynthesis of the nudicaulin skeleton. The question at which biosynthetic stage the glucose (R^1 in Scheme 4) and sophorose (R^2 in Scheme 4) are attached to the nudicaulin skeleton remains to be studied.

The biosynthetic pathway elaborated in this work provides an excellent basis for the identification of the genes and the enzymes that catalyze the fusion of the two key nudicaulin precursors: indole and pelargonidin glycoside.

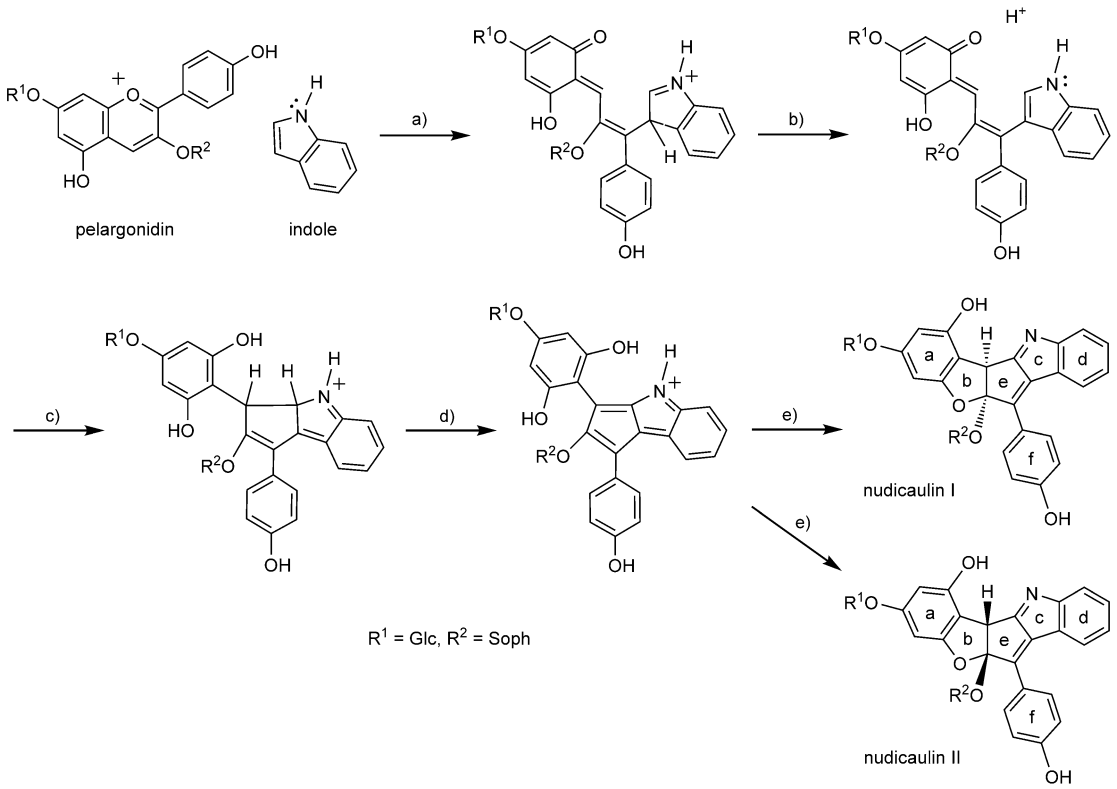

Scheme 4. Hypothetical mechanism for the formation of nudicaulins from indole and pelargonidin. a) C–C bond formation between C-3 of indole and C-2 of pelargonidin proceeds through electrophilic aromatic substitution; b) reconstitution of the aromatic pyrrole ring; c) the C–C bond between C-2 of indole and C-4 of the polyphenol unit is formed through a second electrophilic aromatic substitution; d) dehydrogenation generates a conjugated system consisting of rings c, d, e, and f; e) acetalization closes ring b and generates the diastereomeric aglycone scaffolds of nudicaulins I and II, and deprotonation results in the nudicaulin bases.

Experimental Section

General experimental procedures: Preparative HPLC was performed with a Merck–Hitachi LiChrograph chromatography system (L-6200A gradient pump, L-4250 UV/Vis detector) and with a Shimadzu HPLC (DGU-20A degasser, LC-20AT liquid chromatography pump, SIL-10AP autosampler, CTO-20A column oven, SPD-20A UV detector, FRC-10 A fraction collector) and a Purospher STAR RP18ec column (5 μm, 250×10 mm). For the isolation of nudicaulins (method 1), a linear gradient of MeOH/H_2O (0.1% TFA) from 20% to 50% MeOH over 30 min (flow rate 3.5 mL min^{-1}; UV detection 254 nm) was applied. To monitor the sample preparation steps and the purities of samples, analytical HPLC was performed with an Agilent series HP1100 (binary pump G1312A; auto sampler G1313A; diode array detector G1315B, 200–700 nm) and a Purospher STAR RP18ec column (5 μm, 250×4 mm; injection volume 20 μL). A linear gradient of MeOH/H_2O (0.1% TFA) from 5% to 100% MeOH over 30 min (flow rate 1.0 mL min^{-1}; UV detection 254, 350, and 460 nm) was applied (method 2).

^{1}H and ^{13}C NMR spectra of labeled nudicaulins obtained from [$^{13}C_2$]acetate, [ring-$^{13}C_6$]anthranilic acid, L-[$^{13}C_9$]phenylalanine, and [$^{13}C_6$]glucose were acquired with a Bruker Avance 500 NMR spectrometer (Bruker, Karlsruhe, Germany), operating at 500.13 MHz for ^{1}H and 125.75 MHz for ^{13}C. The spectrometer was equipped with a TCI cryoprobe (5 mm). ^{1}H and ^{13}C NMR spectra of labeled nudicaulin I obtained from [2-^{13}C]indole were acquired with a Bruker Avance III HD 700 NMR spectrometer, operating at 700.45 MHz for ^{1}H and 176.13 MHz for ^{13}C. The spectrometer was equipped with a TCI microcryoprobe (1.7 mm). All samples were measured in CD_3OD, and the residual solvent signals ($\delta = 3.31$ for ^{1}H and $\delta = 49.15$ for ^{13}C) were used as internal chemical shift references. Chemical shifts are given in δ values. The residual HDO signal in the ^{1}H NMR spectra was suppressed by use of the PURGE[21] pulse sequence. ^{13}C NMR spectra were acquired by use of the Bruker "zgpg30" pulse sequence with proton power-gated decoupling (30 degree flip angle, spectral width 28,985 Hz, acquisition time 1.13 s, relaxation delay 2 s).

The UHPLC-MS (ESI) system consisted of an Ultimate 3000 series RSLC (Dionex, Sunnyvale, CA, USA) liquid chromatograph connected to a LTQ Orbitrap XL mass spectrometer (Thermo Fisher Scientific, Bremen, Germany). UHPLC was performed with an Acclaim C18 Column (150×2.1 mm, 2.2 μm, Dionex) at a constant flow rate of 300 μL min^{-1} and use of a binary solvent system [Solvent A, H_2O with HCOOH (0.1%) and solvent B, MeCN with HCOOH (0.1%)]. The HPLC gradient system started with 2% B and increased linearly to 30% B over 10 min, then increased to 90% B over 14 min, was held for 4 min, and was brought back to the 2% B initial condition before being held for 5 min for the column re-equilibration for the next injection (method 3). Full-scan mass spectra were generated with 30000 mΔm^{-1} resolving power. The mass accuracy was better than 3 ppm for MS experiments.

The GC-MS system consisted of an HP6890 (Hewlett Packard) gas chromatograph coupled to an AutoSpec sector field mass spectrometer (Micromass, Manchester, UK). GC was performed with a ZB5HT column (30 m, i.d. 0.25 mm, film thickness 0.25 μm, Phenomenex, Torrance, CA, USA). Inlet 250 °C, temperature regime of the column oven: 60 °C for 2 min, increase at 15 °C min^{-1} to 300 °C, 300 °C for 5 min. Carrier gas: He, flow rate 1 mL min^{-1}. Electron ionization mass spectra (EIMS) were recorded with an ionization energy of 70 eV, mass range *m/z* 40 to 400, splitless injection (1 μL).

Plant material: Seeds of *Papaver nudicaule L.* were obtained from Jelitto Staudensamen, GmbH (Schwarmstedt, Germany), germinated, and grown in soil in the greenhouse facilities of the Max Planck Institute for Chemical Ecology, Jena, Germany. The temperature was 21–23 °C during the day and 19–21 °C during the night. Relative air humidity was between 50% and 60%. The soil was irrigated daily for 10 min. The natural daily photoperiod was supported with 14 h illumination from Phillips Sun-T Agro 400 Na lights.

Labeling experiments: Petals (≈1 g) from closed buds of the yellow-blooming cultivar of *P. nudicaule L.* were sliced and immediately transferred into an aqueous solution (50 mL) containing the labeled substrate and glucose (200 mg). The labeled precursors were administered as follows: [$^{13}C_2$]acetate [15 mg Na^+ salt, 99% ^{13}C, Cambridge Isotope Laboratories (CIL)], [ring-$^{13}C_6$]anthranilic acid (10.5 mg, 99% ^{13}C, Sigma–Aldrich), [$^{13}C_6$]glucose (125 mg, 99% ^{13}C, CIL), [2-^{13}C]indole (10.5 mg, 98% ^{13}C, CIL), L-[$^{13}C_9$]phenylalanine (15 mg, 98% ^{13}C, CIL), [$^{13}C_{10}$]tryptamine (10 mg, 99% ^{13}C, synthesized from L-[$^{13}C_{11}$]tryptophan), L-[$^{13}C_{11}$]tryptophan (15 mg, 99% ^{13}C, CIL), L-[2-^{13}C]tyrosine (10 mg, 99% ^{13}C, CIL). The suspension of the petal tissue was slowly agitated during the average incubation time of 4 days. Then the petals were removed from the incubation mixture by filtration and extracted, after which the nudicaulins were isolated. The retro-biosynthetic analysis of the experiment with [$^{13}C_6$]glucose was carried out as previously reported.[14,22,23] For details, see the Supporting Information.

Extraction of petals and isolation of nudicaulins: Petals of *P. nudicaule* were harvested, lyophilized, ground, and extracted three times with MeOH in an ultrasonic bath. The combined extracts were loaded onto SPE cartridges (Discovery DSC18 SPE, Sigma–Aldrich, 1 g) and eluted with water, MeOH (50%), and MeOH. The MeOH (50%) fraction was dried and then reconstituted in phosphate buffer (10 mM, pH 5.8). Nudicaulins were separated from the flavonoid fraction by use of a strong cationic exchange cartridge (Discovery DSC-SCX SPE Sigma–Aldrich, 1 g). The flavonoid fraction was eluted with MeOH (6 mL), followed by nudicaulin elution with concentrated aqueous NH_3/methanol (1:3, *v/v*, 6 mL). Six out of the eight nudicaulins that have been identified in flowers of *P. nudicaule* exist in the form of acylated glucosides.[11] In order to simplify the structural diversity to that of nudicaulin diastereomers I and II, the acyl units were removed by basic hydrolysis. For this purpose, the fraction was concentrated to dryness and reconstituted in MeOH (50%, 4 mL). NaOH (1 M, 600 μL) was added, and the mixture was stirred for 30 min at room temperature. The hydrolysis was stopped by the addition of glacial acetic acid (100 μL). Afterwards SPE was repeated as described to remove byproducts and buffer residuals. Nudicaulins I and II were isolated by prep. HPLC (method 1) and fully characterized by NMR and MS.

Analysis of indole: Buds of yellow *Papaver nudicaule* were harvested at days 7, 5, 3, 2, and 1 before flowering and were separated from the sepals. Petals of open flowers (day 0) were also harvested. Samples were stored on ice until further treatment. Material from the six samples was ground in liquid nitrogen and extracted with CH_2Cl_2 (600 μL per 0.2 g petals) in gently shaken glass vials for 30 min on ice. The samples were centrifuged for 5 min at 4 °C (0.6 g). The organic phases were used in GC-MS analysis.

PDB experiments: Petals (≈1 g) from closed buds of the yellow-blooming cultivar of *P. nudicaule L.* were sliced and immediately transferred into an aqueous solution (50 mL) containing the labeled substrate and glucose (100 mg). The following potential precursors were administered: 4-fluoroanthranilic acid (2.5 mg, Sigma–Aldrich), 6-fluoroanthranilic acid (2.5 mg, Sigma–Aldrich), 5-hydroxyanthranilic acid (2.5 mg, Sigma–Aldrich), 3-hydroxyanthranilic acid (2.5 mg, Sigma–Aldrich), 5-methylanthranilic acid (2.5 mg, Sigma–Aldrich), cyanidin (5 mg, Sigma–Aldrich), delphinidin (5 mg, Sigma–Aldrich). The suspension of the petal tissue was slowly agitated during the incubation time of 2 d. Then the petals were extracted, and the extracts were treated as described above for the isolation of nudicaulins. Aliquots with concentrations of 40 μg mL^{-1} were analyzed by UPLC-MS (ESI) (extracted ion chromatograms).

Acknowledgements

This work was supported by an FP7 Marie Curie Intra-European Fellowship to E.C.T. (BIOSYN-NUDICAUL project, Contract No. 221274). We thank Dr. Willibald Schliemann for valuable discussions and Emily Wheeler for editorial assistance.

Keywords: biosynthesis · indole alkaloids · isotopic labeling · natural products · nudicaulins

[1] M. Hesse, *Alkaloide: Fluch oder Segen der Natur?* Wiley-VCH, Weinheim, **2000**.
[2] C. Coderch, A. Morreale, F. Gago, *Anti-Cancer Agents Med. Chem.* **2012**, *12*, 219–225.
[3] M. A. Jordan, *Curr. Med. Chem. Anti-Cancer Agents* **2002**, *2*, 1–17.
[4] Y.-J. Wu in *Heterocyclic Scaffolds II: Reactions and Applications of Indoles* (Ed.: G. Gribble), Springer, Berlin, **2010**, pp. 1–29.
[5] T. C. Barden, *Top. Heterocycl. Chem.* **2010**, *26*, 31–46.
[6] S. E. O'Connor, J. J. Maresh, *Nat. Prod. Rep.* **2006**, *23*, 532–547.
[7] K. Miettinen, L. Dong, N. Navrot, T. Schneider, V. Burlat, J. Pollier, L. Woittiez, S. van der Krol, R. Lugan, T. Ilc, R. Verpoorte, K. M. Oksman-Caldentey, E. Martinoia, H. Bouwmeester, A. Goossens, J. Memelink, D. Werck-Reichhart, *Nat. Commun.* **2014**, *5*, 3606.
[8] M. B. Calvert, J. Sperry, *Chem. Commun.* **2015**, *51*, 6202–6205.
[9] T. Kanchanapoom, R. Kasai, P. Chumsri, K. Kraisintu, K. Yamasaki, *Tetrahedron Lett.* **2002**, *43*, 2941–2943.
[10] J. J. Vepsäläinen, S. Auriola, M. Tukiainen, N. Ropponen, J. Callaway, *Planta Med.* **2005**, *71*, 1053–1057.
[11] W. Schliemann, B. Schneider, V. Wray, J. Schmidt, M. Nimtz, A. Porzel, H. Böhm, *Phytochemistry* **2006**, *67*, 191–201.
[12] E. C. Tatsis, H. Böhm, B. Schneider, *Phytochemistry* **2013**, *92*, 105–112.
[13] E. C. Tatsis, A. Schaumlöffel, A. C. Warskulat, G. Massiot, B. Schneider, G. Bringmann, *Org. Lett.* **2013**, *15*, 156–159.
[14] E. C. Tatsis, E. Eylert, R. K. Maddula, E. Ostrozhenkova, A. Svatoš, W. Eisenreich, B. Schneider, *ChemBioChem* **2014**, *15*, 1645–1650.
[15] W. S. Glenn, W. Runguphan, S. E. O'Connor, *Curr. Opin. Biotechnol.* **2013**, *24*, 354–365.
[16] J.-L. Ferrer, M. B. Austin, C. Stewart, Jr., J. P. Noel, *Plant Physiol. Biochem.* **2008**, *46*, 356–370.
[17] T. Vogt, *Mol. Plant* **2010**, *3*, 2–20.
[18] G. Cornuz, H. Wyler, J. Lauterwein, *Phytochemistry* **1981**, *20*, 1461–1462.
[19] R. J. M. Goss, S. Shankar, A. A. Fayad, *Nat. Prod. Rep.* **2012**, *29*, 870–889.
[20] J. R. Price, R. Robinson, R. Scott-Moncrieff, *J. Chem. Soc.* **1939**, 1465–1468.
[21] A. J. Simpson, S. A. Brown, *J. Magn. Reson.* **2005**, *175*, 340–346.

[22] W. Eisenreich, C. Huber, E. Kutzner, N. Knispel, N. Schramek in *The Handbook of Plant Metabolomics* (Eds.: W. Weckwerth, G. Kahl), Wiley-VCH, Weinheim, **2013**, pp. 25 – 56.

[23] W. Römisch-Margl, N. Schramek, T. Radykewicz, C. Ettenhuber, E. Eylert, C. Huber, L. Römisch-Margl, C. Schwarz, M. Dobner, N. Demmel, B. Winzenhörlein, A. Bacher, W. Eisenreich, *Phytochemistry* **2007**, *68*, 2273 – 2289.

Manuscript received: October 26, 2015
Accepted article published: December 16, 2015
Final article published: January 28, 2016

